

## Improved methods for solar Dark Matter searches with the IceCube neutrino telescope

---

### The IceCube Collaboration<sup>†</sup>

<sup>†</sup> [http://icecube.wisc.edu/collaboration/authors/icrc15\\_icecube](http://icecube.wisc.edu/collaboration/authors/icrc15_icecube)

E-mail: [marcel.zoll@fysik.su.se](mailto:marcel.zoll@fysik.su.se)

Gravitationally captured Dark Matter in the form of Weakly Interacting Massive Particles (WIMPs) can annihilate into standard-model particles, such as neutrinos. The IceCube neutrino detector at the South Pole is an excellent instrument to search for such a neutrino signal from the Sun. We present an alternative analysis which improves on previous approaches, in particular in background-dominated regions. Newly developed techniques based on hit clustering and hit-based vetos allow a more accurate reconstruction and identification of events in the detector and thereby a stronger rejection of background. These techniques are also applicable to other IceCube analyses and event filters. We present results for a solar WIMP search using the first year of data taken with the completed IceCube detector with 86 strings.

**Corresponding authors:** Marcel Zoll<sup>\*1</sup>

<sup>1</sup> *Fysikum, Stockholm Universitet, 11419 Stockholm, Sweden*

*The 34th International Cosmic Ray Conference,  
30 July- 6 August, 2015  
The Hague, The Netherlands*

---

\*Speaker.

## 1. Introduction

There is strong observational evidence for the existence of Dark Matter in the universe, including our own galaxy[1], which could possibly have a particle manifestation. Examination of this possibility to date has not revealed the exact constituents of Dark Matter. One intriguing candidate is a Weakly Interacting Massive Particle (WIMP) [2], which could for example emerge in a super-symmetric extension of the Standard Model (SM). If Dark Matter indeed exists in the form of WIMPs, they should reveal their presence through their annihilation into lighter detectable SM particles. Still, with a low local density of about  $0.3 \text{ GeV/cm}^3$  and preferred WIMP masses in the range from a few GeV up to the TeV scale, as well as the cross-section limits obtained, their annihilation processes remain rarely accessible for our observation.

Due to their gravitational interaction, it is probable that WIMPs get gravitationally trapped inside heavy bodies of ordinary matter. The Sun represents the best nearby candidate for this capture process which is driven by the scattering of the WIMPs on nuclei of the Sun, binding them to the system, and subsequent gradual energy losses while sinking towards the Sun's centre. The resultant over-density of WIMPs in a sphere at the centre of the Sun increases the rate of self-annihilation processes so that it is competitive with the capture rate. Considering the lifetime of the Sun, we assume that these processes have reached equilibrium[3]. The annihilations will result in a variety of SM particles, with further particles produced in secondary decay processes, of which only neutrinos can possibly escape the Sun without absorption. The detection of a neutrino flux from the Sun at energies similar to the rest-mass of the WIMP would therefore provide evidence of the presence of Dark Matter and indicate some of its properties.

We present a search for solar WIMPs with the IceCube neutrino telescope. We use one year of data recorded in 2011/12 with the fully completed detector (IC86). A second independent solar WIMP analysis has been carried out on the same data set. It achieved a consistent result and is presented as a separate contribution (ICRC 1209[4]).

## 2. The IceCube Neutrino Detector

IceCube is a cubic-kilometer sized neutrino detector installed in the ice at the geographic South Pole [5] between depths of 1450 m and 2450 m. Detector construction started in 2005 and finished in 2010. The detector consists of an array of 5160 digital optical modules (DOMs) assembled on 86 so-called strings. The DOMs detect the light emitted whenever a neutrino undergoes a neutral current (NC) or charged current (CC) interaction on a nucleus in the ice. Only the CC interaction of a muon neutrino creates an energetic and therefore long-ranged muon, whereas the products of all other interactions lose all their energy in particle showers with a typical size of a few meters. Events in IceCube thus leave two distinct hit patterns in the detector: tracks, identified by the extended pattern of Cherenkov-light emitted as the muon propagates  $O(\text{km})$ , and spherical cascades, caused by particle showers in NC and CC interactions, as well as by stochastic losses along a muon-track, which can dominate in terms of the amount of light emitted. All IceCube analyses reconstruct events recorded in the detector by fits to these two very distinct light distribution patterns.

In IceCube data at trigger level two effects of nuisance are found: detector noise (500-700 Hz per DOM) and event coincidences, where two or more events are simultaneously present inside the

detector ( $\sim 10\%$  of the events). Both effects lead to errors in event reconstructions and need to be removed by algorithms performing *noise/hit-cleaning* and *event-splitting*.

### 3. The IceHive Event-splitter

In this analysis a novel event-splitter named IceHive was developed, which is based on clustering of DOM-hits in space and time with an imposed multiplicity requirement. This clustering routine is based on the determination of whether any two hits are causally connected and are therefore caused by a common source of light (*physics hit*), different from stochastic noise (*noise hit*). Collecting physics hits into clusters while excluding noise hits allows the separation of individually developing sub-events in the detector.

The relation between two physics hits can be described by one of the following causes:

1. hits are located on different geometrical/topological sites of the same light-front (Cherenkov-cone), thus are spatially separated with no or little time separation
2. hits are caused by photons of the same light-front travelling between DOMs, thus hits are connected by the speed of photon propagation
3. hits are caused by light-emission at different positions along a muon-track, thus hits are connected by the speed of particle propagation

A graphical impression of this can be found in Figure 1.

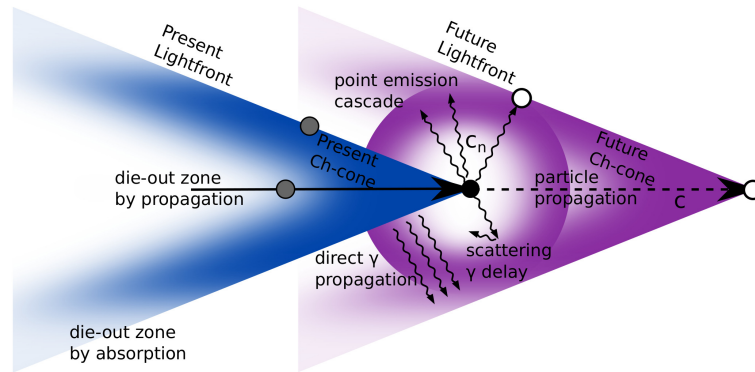


**Figure 1:** Possible light emission topologies for tracks and cascades at the present (blue) and future (pink) after photon-propagation for a particle (arrow) traversing the detector volume. Hits are registered on DOMs (circles); their relation is governed by the causal arguments of spatial separation, photon propagation and particle propagation.

This allows the construction of a binary causal connection estimator between hits  $h_1(\vec{r}_1, t_1)$  and  $h_2(\vec{r}_2, t_2)$  with three dedicated terms (without restriction of generality:  $t_1 < t_2$ ):

$$E(h_1, h_2) = [(h_2 \in EV_{\text{static}}(h_1)) \wedge (\alpha_{\infty}^- \leq R_{\infty}(h_1, h_2) \leq \alpha_{\infty}^+)] \quad (3.1)$$

$$\vee [(h_2 \in EV_{\text{photon}}(h_1)) \wedge (\alpha_{\text{cice}}^- \leq R_{\text{cice}}(h_1, h_2) \leq \alpha_{\text{cice}}^+)] \quad (3.2)$$

$$\vee [(h_2 \in EV_{\text{particle}}(h_1)) \wedge (\alpha_{\text{vac}}^- \leq R_{\text{vac}}(h_1, h_2) \leq \alpha_{\text{vac}}^+)] \quad (3.3)$$

where  $R_v = (t_1 - t_2) - |\vec{r}_1 - \vec{r}_2|/v$  is the time-residual of a messenger particle travelling with speed  $v$  between hits, the  $\alpha_v^\pm$  are adjustable parameters, and  $EV_{\text{relation}}$  is the eligibility volume (EV) containing all DOMs to which a specific hit can possibly connect. The EV needs to be selected according to the typical range of the messenger and the imposed multiplicity criterion. In contrast to previous solutions IceHive explicitly takes the detector geometry into account when the EV is constructed<sup>1</sup>. These equations with careful selection of the involved parameters make IceHive very robust against the influence of noise, so that its application on the raw detector readout becomes possible. Figure 2 shows the ability of IceHive to select the correct physics hits. Applied before online reconstructions and filters, IceHive could demonstrate an additional background reduction of 30% for muon topologies and 65% for cascades. Coincident events, which are expected to be found at an abundance of 10% in the recorded data, were separated at a success rate of 87%.

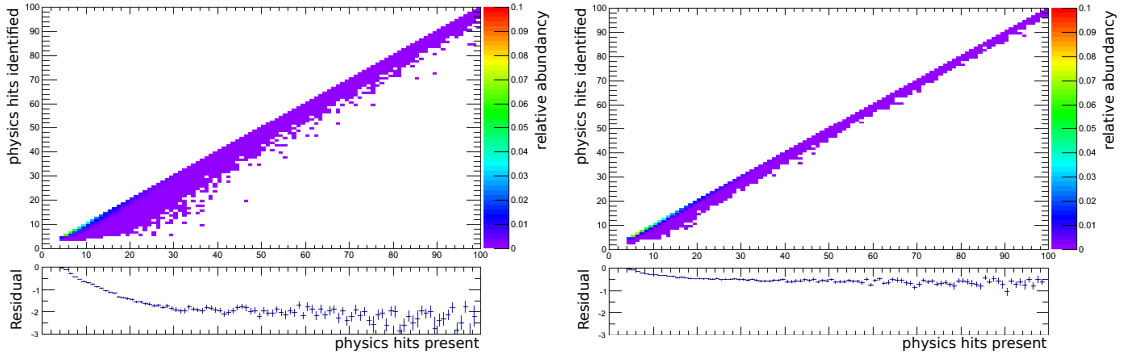


**Figure 2:** Comparing the selection of physics hits for the previous event-splitter solution based on spatial clustering (left) and the improved IceHive algorithm (right). Optimal performance is indicated along the diagonal. The residual plots show the average number of missed physics hits for events with different number of physics hits present in total.

#### 4. Event Selection

For this analysis we produce dedicated signal simulation using WimpSim [6, 7] for several WIMP masses. We pick the annihilation into  $W^+W^-$  and  $\tau^+\tau^-$  to represent a hard neutrino spectrum and annihilation into  $b\bar{b}$  for a soft one and thereby bracket other conceivable branching scenarios. Depending on the WIMP mass and annihilation channel, the expected signal neutrinos at the detector range in energy from just a few GeV up to some TeV. This analysis focuses exclusively on a signal in muon neutrinos creating tracks in the detector, as these in general yield the best pointing. Compared to previous WIMP analyses in IceCube, the detector simulation has been substantially improved; in particular, the description of the particle/photon propagation and detection in ice, as well as the detector response.

The regular IceCube (IC) array has a threshold on the neutrino energy  $\sim 100$  GeV while the more densely instrumented region DeepCore (DC) lowers this threshold to  $\sim 10$  GeV. All IceCube neutrino analyses suffer from a strong background of down-going muons and neutrinos created

<sup>1</sup>The detector geometry resembles regular hexagons similar to a bee hive, hence the naming of the algorithm.

from cosmic ray showers in the upper atmosphere. Atmospheric muons will be observed only as down-going while atmospheric neutrinos are found at all directions. This greatly influences the approach to the event selection.

As the event-splitter IceHive shows better performance compared to the methods used traditionally, it is initially applied to all available detector data selected by any of the online filters ( $\sim 800$  Hz) during one year of live-time (337.4 d). Thereafter event reconstructions are performed on the split physics hit selection and minimum quality cuts are enforced.

The event sample is then split into four sub-samples: if the hits of an event are predominantly found in the denser instrumented region of DeepCore they are classified as *DC-dominated*, otherwise they are classified as *IC-dominated*. Another subdivision is performed according to the incident zenith angle, where events originating from above the horizon are dominated by through-going atmospheric muons (referred to as *BG-dominated*).

In the further treatment we require that events in the BG-dominated sample are starting within the detector, which can only be fulfilled by true neutrino events; the detector's outer layer of strings act as an active veto. No such requirement is applied for the up-going (not BG-dominated) sample, because the Earth acts as a natural filter for the atmospheric muon background.

At this level of about 1 Hz we apply two dedicated Boosted Decision Trees (BDT), one for DC-dominated and another one for IC-dominated events, thus the different background samples are treated conjointly. These BDTs are trained solely on variables expressing the containment of events in the detector, thus explicitly ignore any energy dependence. This reduces the background by another factor of  $\sim 10$ . Thereafter another four now energy-sensitive BDTs are applied, one to each of the four sub-samples. The second stage BDTs are trained on a signal sample which is typical for the respective selection: 1 TeV WIMPs annihilating into  $W^+W^-$  for the IC-dominated samples and an equal mixture of 100 GeV WIMPs into  $W^+W^-$  and  $b\bar{b}$  and 50 GeV WIMPs into  $\tau^+\tau^-$  for the DC-dominated samples. The BDT-classifiers at this point are sensitive to the specific energy spectrum and zenith distribution of the signal expectation and can now be used as tuning parameters. Figure 3 shows the classifier distributions for the up-going subsamples. A loose cut on the BDT-classifier at zero brings the data rate down to about 20 mHz.

Up to this level the background has been reduced by a factor of  $4 \cdot 10^4$  while, depending on chosen mass and annihilation channel, between 11% and 20% of the signal could be retained.

## 5. Analysis method

We use a shape likelihood based on the opening angle  $\Psi$  of the observed event direction compared to the current position of the Sun. The probability density function for an event  $\vec{e}_i$  as a set of observable quantities in a sample containing  $\mu$  signal events in a total of  $N_{\text{obs}}$  events is given by

$$g(\vec{e} = (\Psi)|\mu) = \frac{\mu}{N_{\text{obs}}} f_s(\Psi) + \left(1 - \frac{\mu}{N_{\text{obs}}}\right) f_{\text{bg}}(\Psi) \quad (5.1)$$

where  $f_s(\Psi)$  and  $f_{\text{bg}}(\Psi)$  are the probability distribution function (PDF) for signal and background. The signal PDF can be obtained by direct tabulation from WIMP simulation of any specific mass-channel combination; in contrast the background PDF is obtained from experimental data by scram-

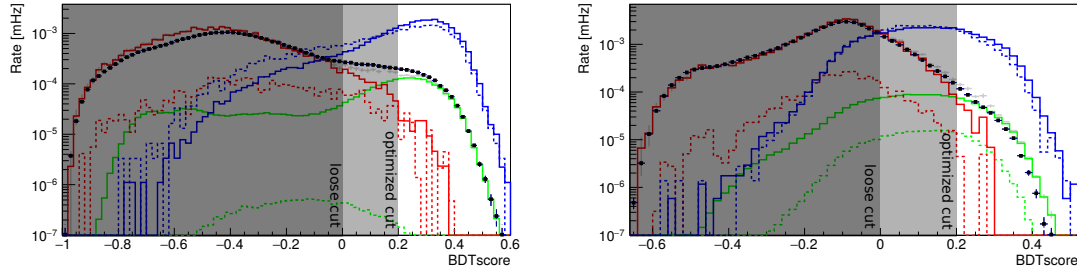


**Figure 3:** The energy-sensitive BDT-classifier score for the up-going subsamples of IC-dominated (left) and DC-dominated events (right). Events scored to high values are most signal-like. Shown is experimental data (black) and the simulation of atm.  $\nu_\mu$  (solid green) and atm.  $\nu_e$  (dashed green), as well as atm.  $\mu$  from CORSIKA at low (solid red) and high primary energies (dashed red). The simulation total is shown in gray. The signal expectation (blue) scaled to the data-rate is shown for a representative of a hard (solid) and soft (dashed) spectrum in the respective sample.

bling the apparent Sun azimuth, thereby removing any possible signal traits in  $\Psi$ ; see figure 4 for some examples.

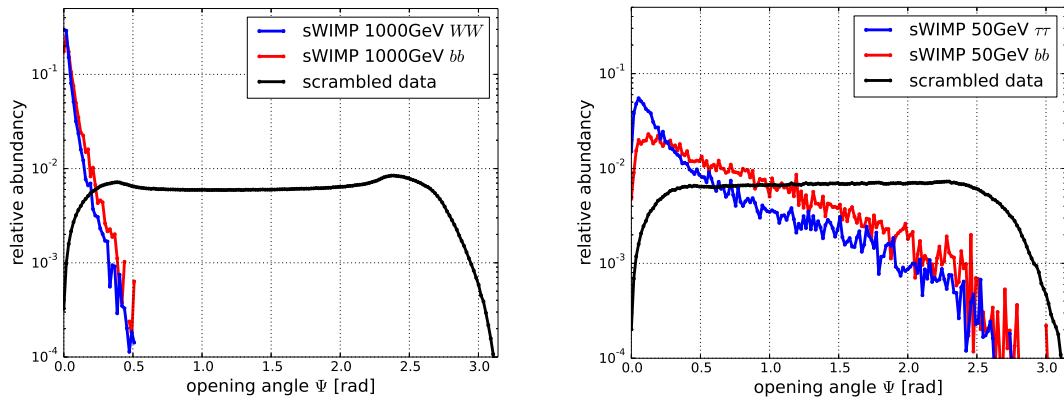


**Figure 4:** The obtained PDFs for background by scrambled experimental data and a hard and soft signal expectation in the IceCube-dominated (left) and DeepCore-dominated (right) sample. Only the winter months and up-going events are considered. The different structure in the background is caused by selection and geometrical effects in the respective sample.

The likelihood value for  $\mu$  signal events in the complete sample is then given by

$$\mathcal{L}(\mu) = \prod_i^{N_{\text{Obs}}} g(\vec{e}_i | \mu) \quad (5.2)$$

We use the prescription from Feldman and Cousins[8] to construct a test statistic and extract sensitivities and limits for the number of observed signal events in the sample at 90% confidence level. This number can then be converted to a WIMP annihilation rate in the Sun and finally to a limit on the WIMP-nucleon scattering cross-section.

In the evaluation of our data sample, we limit ourselves to data obtained in the winter months (174 days of live-time) when the Sun is below the horizon and all sensitivity is obtained from up-going neutrino events. Furthermore we tighten the last cut on the BDT-classifier to obtain the best

sensitivity from the respective sample. The final event rate is 1.4 mHz in the IC-dominated sample and 0.4 mHz in the DC-dominated sample.

## 6. Results and discussion

This analysis found no significant excess in muon neutrinos from the direction of the Sun in the search for a possible solar WIMP signal. This allows us to set stringent limits on the muon neutrino-flux from the Sun for energies in the GeV-TeV range. Under the assumption of a local DM density at  $0.3 \text{ GeV/cm}^3$ , a standard Maxwellian velocity distribution in the galactic WIMP halo and the Standard Solar Model this limit can be converted to a limit on the WIMP-nucleon scattering cross-section for each such probed WIMP model. Figure 5 shows the obtained sensitivities and limits of this analysis for the spin-dependent and spin-independent scattering cross-section.

Compared to the previous IceCube solar WIMP analysis[9] conducted with 79 deployed strings, the improvement ranges from a factor up to 10 at the lowest WIMP mass at 20 GeV to a factor 2 for higher WIMP masses up to 10 TeV. The improvement over just the added detector volume can be attributed to the refinement of the analysis methods and a better hit selection with IceHive. The so obtained limits make IceCube very competitive compared to the reported limits from other experiments for WIMP masses above  $\sim 150 \text{ GeV}$ .

Note: We have carried out a second independent solar WIMP analysis on the same dataset. The results of the two analyses are consistent with each other and are described as separate contributions to this conference (see [4]). At a later time we will combine the two analyses.

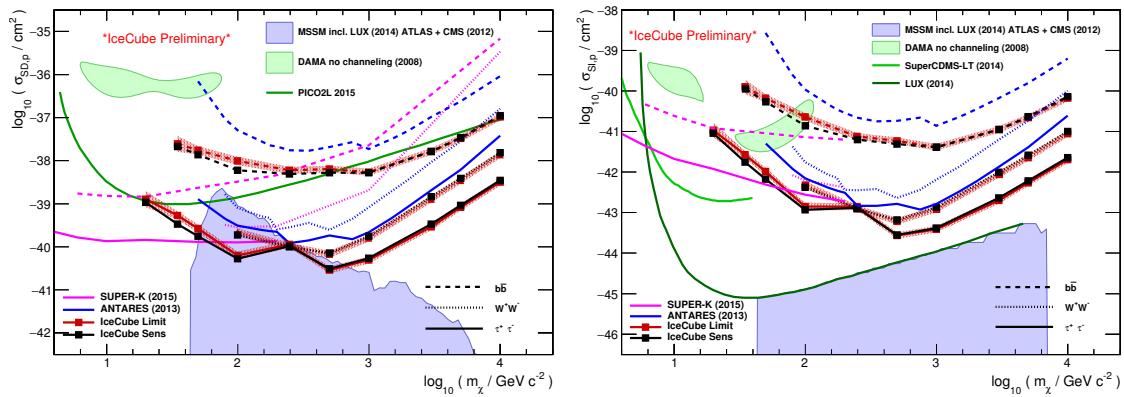


**Figure 5:** Limits of this analysis on the spin dependent (left) and spin independent (right) WIMP-nucleon scattering cross-section as a function of the WIMP mass derived from this analysis. Systematic uncertainties are shown as a red band. Also shown are reported limits from other experiments [10, 11, 12, 13, 14, 15, 16, 17, 18].

## References

- [1] M. Pato, F. Iocco, G. Bertone, Nature 11 (2015) p.245-248
- [2] G. Bertone *et al.*, Phys. Rep. 405 (2005) p.279
- [3] K. Choi *et al.*, JCAP 05, 049 (2014)

- [4] IceCube Coll., PoS(ICRC2015)1209 these proceedings
- [5] A. Achterberg *et al.*, [IceCube Coll.], *Astropart. Phys.* 26 (2006) 155
- [6] M. Blennow, J. Edsjö and T. Ohlsson, *JCAP* 01, 021 (2008), <http://www.fysik.su.se/~edsjo/wimpsim/>
- [7] P. Gondolo, J. Edsjö, P. Ullio, L. Bergström, M. Schelke and E.A. Baltz, *JCAP* 07, 008 (2004)
- [8] G.J. Feldman, R. D. Cousins, *Phys. Rev. D* 57:3873 (1998)
- [9] M.G. Aartsen *et al.* [IceCube Coll.], *Phys. Rev. Lett.* 110, 131302 (2013)
- [10] D.S. Akerib *et al.* [LUX Coll.], *Phys. Rev. Lett.* 112, 091303 (2013)
- [11] R. Agnese *et al.* [SuperCDMS Coll.], *Phys. Rev. Lett.* 112, 241302 (2014)
- [12] R. Bernabei *et al.*, *Eur. Phys. J. C* 53 (2008), 205
- [13] H. Silverwood *et al.*, arXiv:1210.0844v1 (2012)
- [14] The ATLAS Collaboration, *Phys. Lett. B* 701 (2013) 186
- [15] The CMS Collaboration, arXiv:1207.1798 (2012)
- [16] K. Choi *et al.* [Super-Kamiokande Coll.], *Phys. Rev. Lett.* 114, 141301 (2015)
- [17] C. Amole *et al.* [PICO Coll.], *Phys. Rev. Lett.* 114, 231302 (2015)
- [18] The ANTARES Collaboration, *JCAP* 11 (2013) 032